

# Experimental study of the wall surfaces' roughness influence on the hydrodynamics' instabilities in a Couette-Taylor flow

**Lamia Gaié <sup>a</sup>, Emna Berrich-Betouche <sup>b</sup>, Maxence Bigerelle <sup>a</sup>  
and Fethi Aloui <sup>\*a</sup>**

<sup>a</sup> LAMIH CNRS UMR 8201, Département de Mécanique, Université de Valenciennes et du Hainaut-Cambrésis (UVHC), Campus Mont Houy, 59313 Valenciennes Cedex 9 - France

<sup>b</sup> LUNAM Université, Université de Nantes, CNRS, GEPEA, UMR6144, Institut Mines-Télécom, 4 rue Alfred KASTLER - BP20722 44307 Nantes Cedex 03 - France

\* Corresponding author: [gaiedlamia@gmail.com](mailto:gaiedlamia@gmail.com)

## Abstract:

The Couette-Taylor flow starts with a laminar azimuthal state at low rotational speed, going to an intermediate regime by increasing rotational speed with counter-toroidal cells (first instability or Taylor Vortex Flow). Beyond a critical value of rotational speed, various wavy modes break out first, then the flow becomes turbulent. The onset of instabilities depends on the geometry of the system which we use. The aim of this study is to characterize the instabilities (Ta) then to study the effect of surface roughness on the hydrodynamic structures of Couette-Taylor Flow. So different surface conditions for inner cylinder were analyzed: smooth, sandpaper P180 and canvas plastic with different size-mesh.

Characterizing the Couette-Taylor flow, a transition point (TVF to WVT) (WVF to MWVF) (MWVF to TTVF) was found to be influenced by surface roughness.

For this, a qualitative study using reflecting kalliroscope particles was developed to visualize different flow regimes (Taylor vortex flow, wavy vortex flow, modulated wavy vortex flow and turbulent flow) in both smooth and rough walls. Then a quantitative study is investigated. The results showed that the surface roughness has an effect on the appearance of the instability of Taylor.

**Keywords:** Taylor-Couette Flow, roughened surface, Visualization by kalliroscope particles.

## Nomenclature

d	Gap (m)
h	Height (m)
P	Pressure (Pa)
R <sub>1</sub>	Inner cylinder radius (m)
R <sub>2</sub>	Outer cylinder radius (m)
t	time (s)
Ta	Taylor number

$Ta_{c1}$	critical Taylor number
$V$	Velocity (m/s)
Greek symbols	
$\Gamma$	Aspect ratio (h/d)
$\eta$	Radial ratio ( $R_1/R_2$ )
$\nu$	Viscosity (m <sup>2</sup> /s)

## 1. Introduction

The simplicity of the Couette-Taylor systems has encouraged the researchers and the industrials to investigate in this kind of systems. This subject were studied since almost 100 years, firstly by Taylor in 1923 [1].

The Couette-Taylor flow is often observed in various types of engineering applications. For example, as journal bearing lubrication, reactors and bioreactors and on the filtration process reactors for water treatment [2-4].

This subject has kept inspiring researchers and industrials. Till now, more than 2,000 papers have been published. This model has a variety of challenges with complex structures. In fact, it is the first model that provides the appearance of hydrodynamic instabilities and describes the properties of vortex structures (the impact on mass transfer, interaction with the wall, size and energy).

A dimensionless parameter expressing the ratio between the viscous dissipation and the centrifugal force called Taylor number (Ta), is defined to characterize this critical condition.

Later than the first experimental works of Couette [5] devoted to the viscosity measurement, Taylor, combining the theoretical and experimental approach, designed its own device closely according with the hypothesis of infinitely long cylinders. He showed that with small perturbations of the velocity and pressure fields, the viscosity stabilizes the flow at low rotational speeds using linear stability analysis. A dimensionless parameter expressing the ratio between the viscous dissipation and the centrifugal force called Taylor number (Ta), is defined to characterize this critical condition.

By increasing Taylor number (Ta), a sequential transition (*CF to TVF*) (*TVF to WVT*) (*WVF to MWVF*) (*MWVF to TTVF*) was observed. During this transition sequence, the flow keeps a considerably clear temporal and spatial periodicity. In fact, a roll structure of TVF persists all through and remains even in turbulent regime.

Up to now, several experimental, theoretical and recently numerical studies have been dedicated to this problem, and particularly to the Taylor vortices [6-10].

In the present work, a new geometric parameter is introduced to study its effect on the generation of Taylor instabilities. A rough surface is then placed on the wall of the inner cylinder to analyze the influence of surface roughness on flow regimes and the development of vortices.

The idea is to approach the case of lubricating fluid circulating in the hydrodynamic bearings which are often used in systems that operate at a very high speed. The surface condition of the bearings is a very important factor influencing the effectiveness of lubrication. Therefore, the presence of roughness leads to changes the flow regime of lubricant film.

An experimental set up was designed to study the Couette-Taylor flow, to undertake the modelling of the lubricants' flow in hydrodynamic bearings and thus to determine the effect of surface roughness on the instabilities regimes' transition. So, the Taylor number and wavelength of the flow are investigated from laminar to turbulent flow regime and compared to the case of a Taylor Couette flow with a smooth surface, in order to highlight the effect of the roughness on the stability and the behavior of the flow.

For this reason, firstly a qualitative study using reflecting kalliroscope particles was developed to visualize the different flow regimes in both smooth and rough walls.

## 2. Materials and methods

As shown in figure 1, the experimental system consists of two vertical coaxial cylinders made of transparent Plexiglas. The test-section is composed of a rotating inner cylinder (radius  $R_1=85.5$  mm) and a fixed outer cylinder (radius  $R_2=100$  mm). Thus, the radius ratio is  $\eta = R_1/R_2 = 0.97$ . The height of the fluid between the two cylinders is  $h=450$  mm, which results in an aspect ratio of  $\Gamma=h/d=150$ .

The inner cylinder is driven by a  $\alpha$ -step motor with a variable speed. Its maximum speed is 120 rpm. The revolutions were controlled by a speed controller, ensuring any kind of movement (continuous rotation, sinusoidal movement, etc.) for the inner cylinder.

This motor have almost linear characteristics with its rotational speed, being determined by an applied direct voltage.

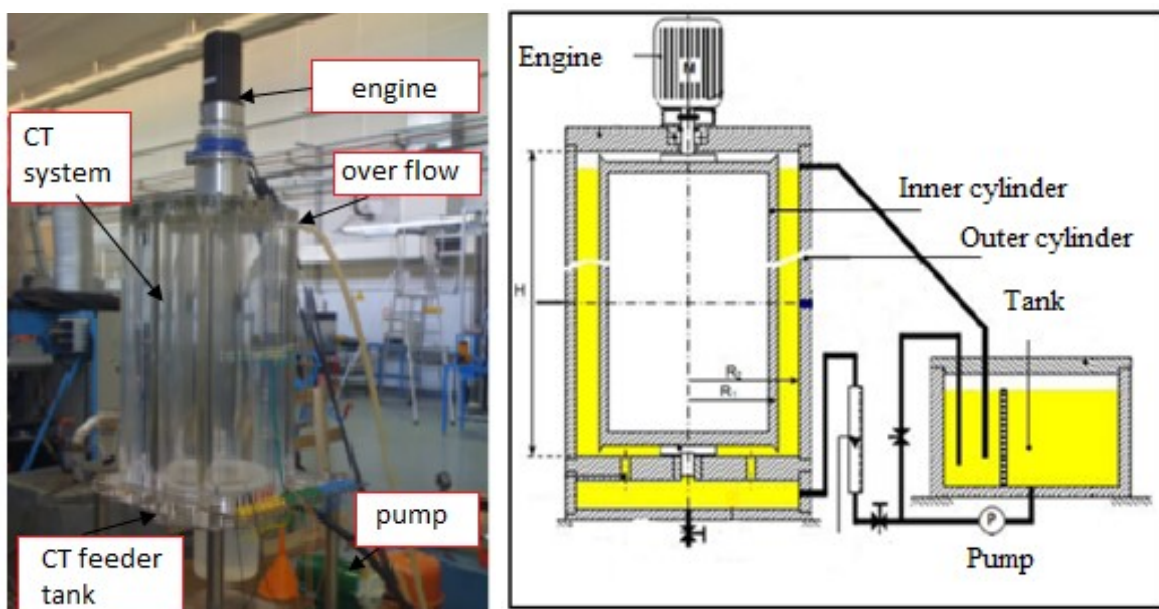


Figure 1: Experimental installation.

### 2.1. Kaliroskopie technique

For the visualization of the flow, kalliroscope particles (which are composed of reflective flakes of flat and elongated shape) were used. These particles are anisotropic, their dimensions are  $30\mu\text{m} \times 6\mu\text{m} \times 0.07\mu\text{m}$ . They ensure a good visibility of the flow even in a small proportion with refractive index ( $n=1.85$ ). To get a cut in the azimuthal plane at the annular space between the two cylinders a laser source KEYLIGHT green type of a wavelength equal to 530nm is used. A CCD camera placed in front of the laser layer provides the images of the flow making it possible to observe the evolution of the instabilities occurred in time.

## 3. Results

### 3.1. Smooth surfaces

#### 3.1.1. Steady Taylor Vortex Flow (TVF)

The Taylor number is used to characterize the flow transition. It describes the competition between the viscous dissipation and the centrifugal force. It is defined as:

$$Ta = \frac{\Omega R_1 d}{\nu} \sqrt{\frac{d}{R_1}} \quad (1)$$

Where  $\Omega$  is the inner cylinder rotational speed.

The velocity gradient is almost constant. The flow regime is thus laminar. It corresponds to the Couette flow regime. The flow is then stable and no vortices appear.

Figure 2 represents the distribution of particles on a longitudinal section of the annular space in the (r,z) plane. The distribution of particles is then homogeneous and uniform along the rotational axis.

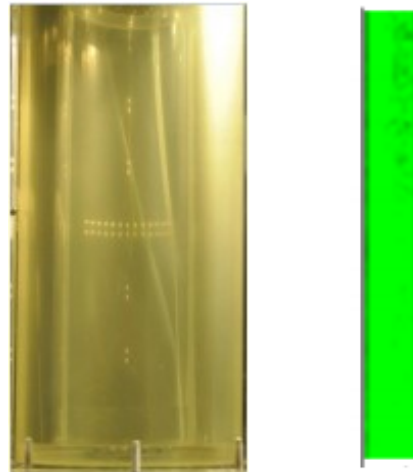


Figure 2: Visualization by kalliroscope of a laser cutting of the annular space at  $Ta=21.9$ .

### 3.1.2. Taylor Couette Flow

The vortex of Taylor appears at  $Ta_{cl}=41.3$  for an inner cylinder with smooth wall (appearance of rings). These vortices of Taylor are characterized by their axisymmetric toroidal shape. This regime extends until  $Ta=52.9$ , which is in agreement with the transition point predicted by Sobolik et al. [11] of  $Ta_{cl}=42.1$ .

Figure 3 represents the distribution of particles at  $t=90s$  for different numbers of Taylor. Taylor Vortices are characterized by an axial periodicity of wavelength  $\lambda$ . Experimentally, the wavelength  $\lambda$  is equal  $\lambda=5.8mm=1.93d$ .

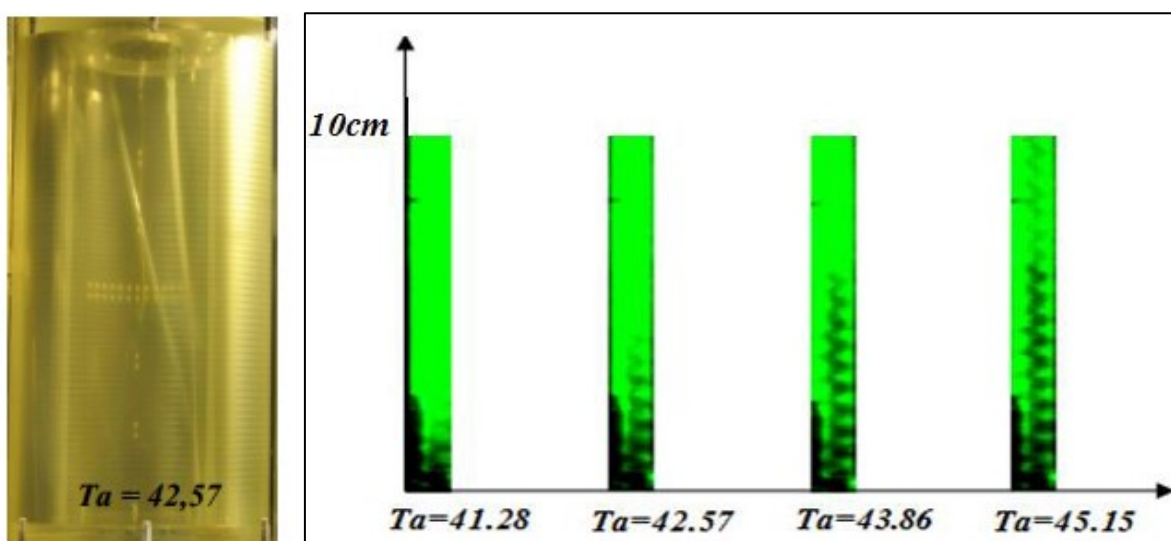


Figure 3: Evolution of the onset of the Taylor vortices in a laser sheet intersecting the annular space.

### 3.1.3. Wavy Vortex Flow (WVF)

By increasing the rotational speed of the inner cylinder, a second flow bifurcation appears at  $Ta=Ta_{c2}=52.98$ . The TVF becomes unstable and is replaced by wavy vortex flow (WVF). Beyond a certain threshold value, the system undergoes a new kind of centrifugal instabilities: a non-axisymmetric instabilities, which lead to a great spatio-temporal complexity, known as wavy vortex flow. This flow state is characterized by an axial wavelength  $\lambda$ , an azimuthal wave number noted  $m$  and a frequency  $f$ .

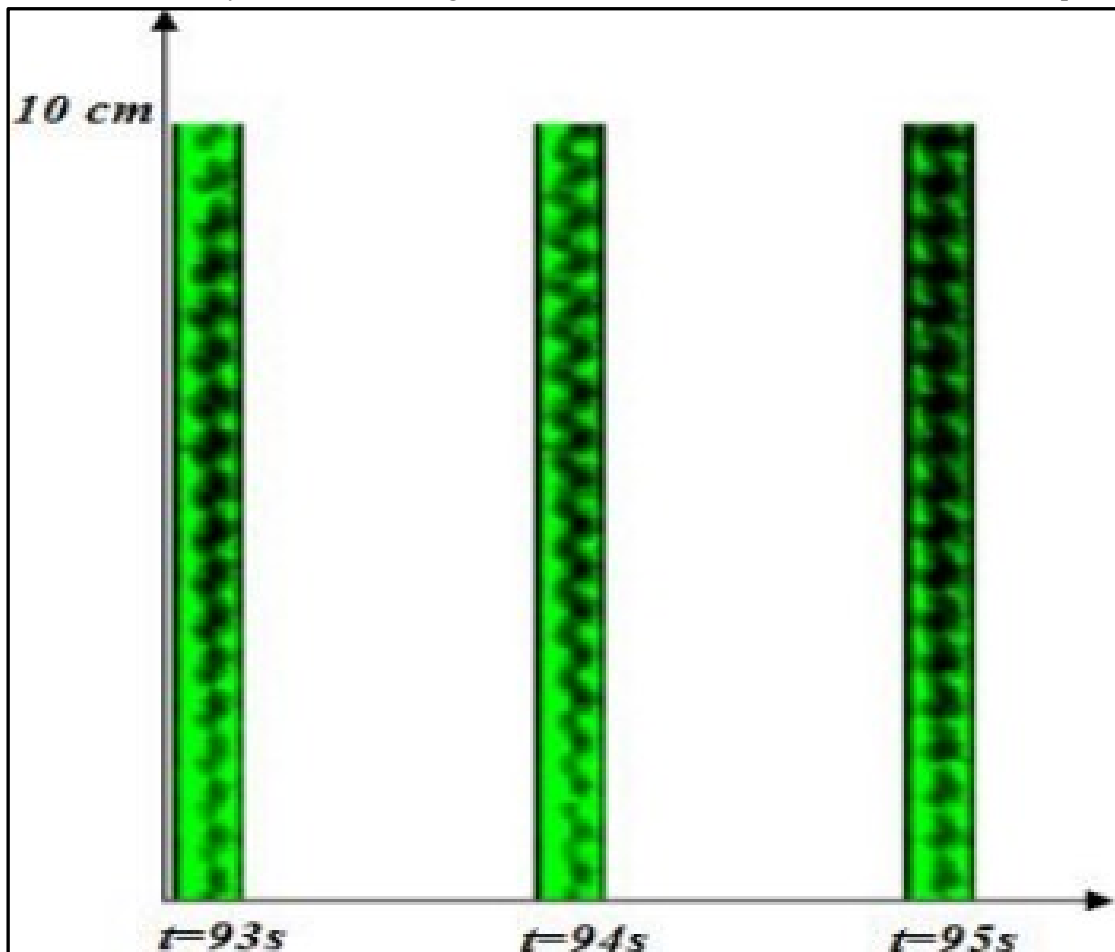


Figure 4: Visualization of the evolution of instabilities in a WVF regime  $Ta = 53$ .

### 3.1.4. Modulated wavy vortex Flow (MWVF)

As  $Ta$  is increased even higher, the amplitude of the azimuthal waves begins to vary with time, giving rise to a quasi-periodic regimes known as modulated Wavy Vortex flow (MWVF) which detected at  $Tac3 = 61.9$  (Figure 5). The vortices begin then to be unstructured.

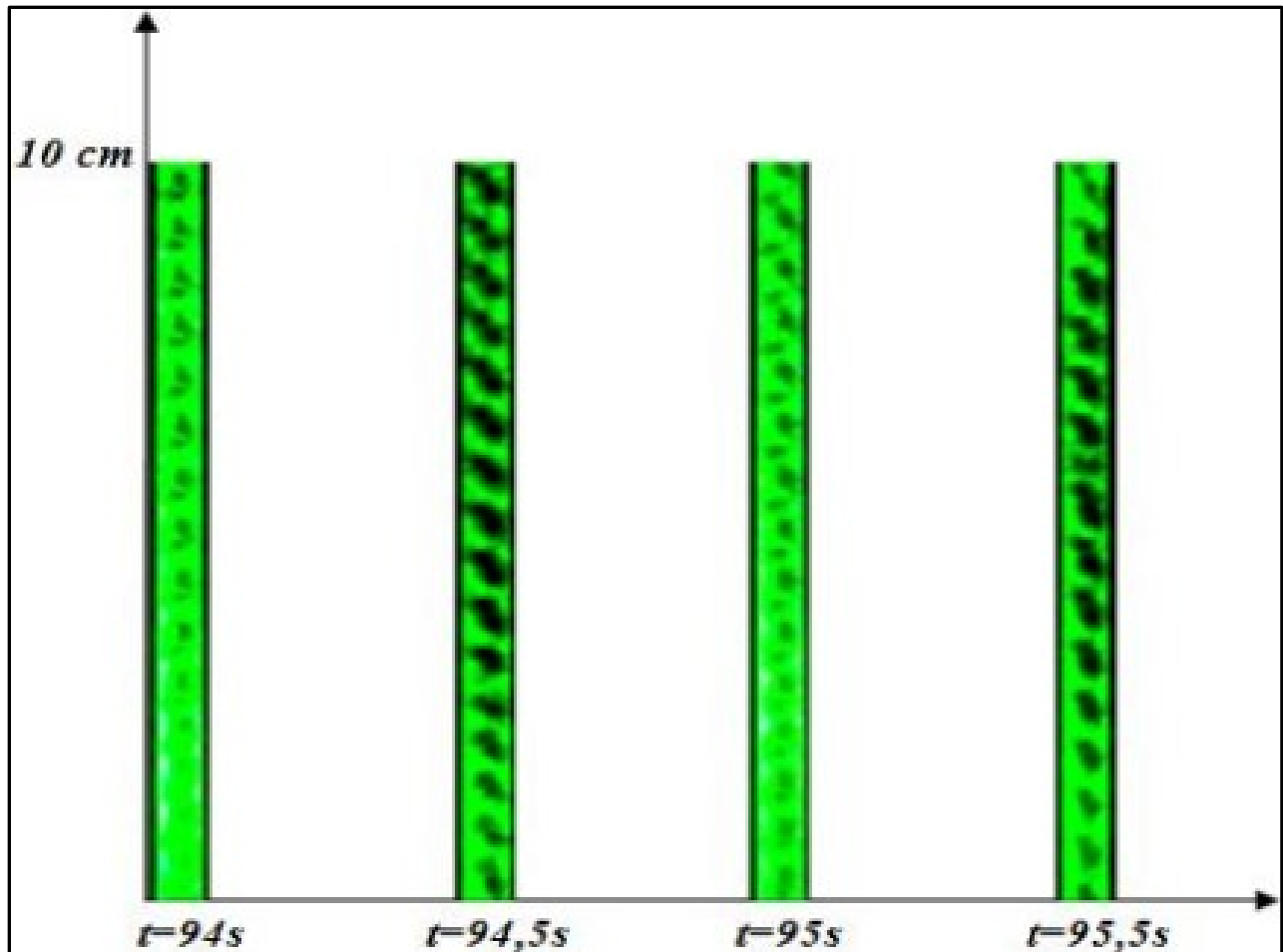


Figure 5: Visualization of the flow instabilities in a MWVF regime  $Ta = 61.9$ .

### 3.1.5. Turbulent Taylor Vortex Flow (TTVF)

On further increasing  $Ta$ , beyond a critical value  $Ta_c=Ta_{c3}=210$ , the azimuthal waves disappear and the flow becomes turbulent (TTVF) as soon as the velocity field has a chaotic structures (turbulent structures) (Figure 6).

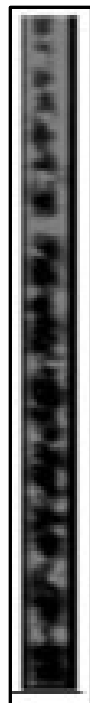


Figure 6: Visualization by kalliroscope of the turbulent regime  $Ta = 210$ .

### 3.2. Rough surfaces

Different surfaces conditions of the inner wall of the cylinder are considered to study its effect on the appearance of instabilities (table 1 below).

Table 1: Characteristics of the different rough surfaces

<i>Sandpaper P180</i>	<i>Canvas plastic1</i>	<i>Canvas plastic2</i>
Average particle Size = $82 \mu\text{m}$	Gap width= $2 \text{ mm}$ Thickness ( $e$ ) = $300 \mu\text{m}$	Gap width = $1 \text{ mm}$ Thickness ( $e$ ) = $500 \mu\text{m}$

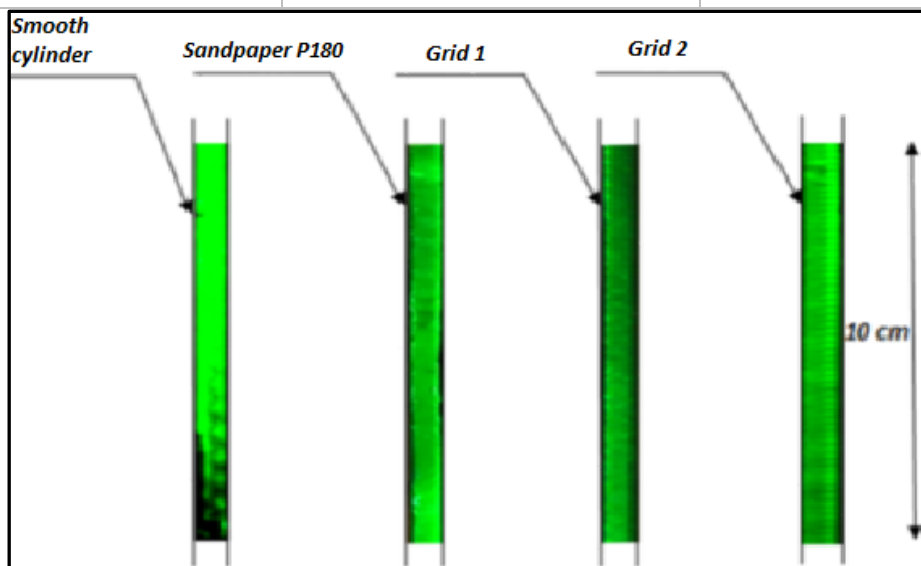


Figure 7: Visualization of the flow instabilities at  $Ta = 42.6$  for different roughness surfaces

Figure 7 shows a perpendicular section of the annular space at Taylor number  $Ta = 42.6$  for different surfaces conditions. As for the onset of TVF, it can be observed that it strongly depends on the surface conditions.

When the surface of the inner cylinder is smooth, the Taylor vortices appears at  $Ta = 42.8$ . Whereas for other rough surfaces the flow remains still stable.

With increasing roughness (plastic canvas), the onset is afterward. For the first plastic canvas, it already starts to form vortices at  $Ta = 47.0$  and with the second plastic canvas, it appears at  $Ta = 47.5$ .

The roughness causes then a delay on the appearance of the first instabilities. This delay has a direct relationship with the size of the roughness.

In effect, the flow will be subjected to friction in contact with the inter cylinder. This friction will result in a reduction in the velocity of the fluid particles. As a result, we can note that the Taylor vortices will be formed late due to the roughness. In opposition, the onset of WVF is less influenced by the surface roughness. Here, smooth, P180 and the first plastic canvas have similar onsets of  $Ta = 52.9, 52.3$  and  $52.4$ .

It can be noted from these results that the onset of the first instabilities (TVF) is influenced by the irregularity of the surface. The rough surface postpone then the flow instabilities. In contrast, for the second instability (WVF) the rough surface triggers the flow instabilities.

Once Taylor cells appears, roughness has no longer any damping effects. On the contrary, it favors the flow disturbance. Therefore, we will have a more rapid change from one regime to another.

Below, table 2 summarizes the different Taylor transitions' regimes, corresponding to each flow regime for various rough surfaces used.

Table 2: Different Taylor transitions for the different rough surfaces used

	<b>Smooth cylinder</b>	<b>Sandpaper P180</b>	<b>Canvas plastic1</b>	<b>Canvas plastic2</b>
<b>TVF</b>	41.3	44.7	47.0	47.5
<b>WVF</b>	52.9	52.3	52.4	55.4
<b>MWVF</b>	61.9	60.8	60.7	58.8
<b>TTVF</b>	210.0	214.7	220.2	197.8

## 4. Conclusions

This paper presents an experimental study on the surface roughness effects on the onset of Taylor instabilities. For this aim, we used different types of roughness surfaces (sandpaper type P180 and 2 plastic canvas). The experimental results showed that a transition point (TVF to WVT, WVF to MWVF and MWVF to TTVF) depends on the size of the surface roughness. The onset of TVF is then strongly influenced by the rough surface. In fact, the surface friction has a direct influence on the surface roughness. The fluid particles' velocity decreases and the first instabilities appear with a delay, by increasing the friction of the surface. In opposition, once the Taylor vortices are created, the roughness has not a damping effect on the flow. We will have a more rapid switching from one regime to another. These results have an enormous impact on the application of Couette-Taylor system, where a rough surface is introduced on the moving wall in contact with the flow.

## Acknowledgments

This work was supported by the laboratory LAMIH CNRS UMR 8201 (University of Valenciennes), Department of Mechanical Engineering. This supports is gratefully acknowledged.

## References

- [1] Taylor G. I., Stability of a viscous liquid contained between two rotating cylinders. *Philosophical Transactions of the Royal Society of London A: Mathematical, Physical and Engineering Sciences* 223, 289-343. (1923).
- [2] Kataoka K., Okubo M., Emulsion polymerization of styrene in a continuous Taylor vortex flow reactor, *Chem. Eng. Sci.*, Vol. 50, 1409-1416 (1995).
- [3] Janes D.A., Thomas, N.H., Callow, J.A., Demonstration of a bubble free annular—vortex membrane bioreactor for batch culture of red beet cells, *Biotechnology Techniques* 1 Vol. 4, 257 (1987).
- [4] Holeschovsky U.B., Conney C.L., Quantitative description of ultrafiltration in a rotating filtration device, *A.I.Ch.E. Journal*, 37 (8), 1219-1226 (1991).
- [5] Couette M., Études sur le frottement des liquides, *Ann. Chim. Phys.* 6, Ser. 21, 433-510 (1890).
- [6] Diprima R.C., Eagles P.M, NG. B.S., Effect of radius ratio on the stability of Couette flow-Taylor vortex flow, *Physics of Fluids*, 27, 2403-2411 (1984).
- [7] Lueptow R.M., Docter A., Min K., Stability of axial flow in an annulus with a rotating inner cylinder, *Phys. Fluids*, 4, 2446 (1992).
- [8] Mahamdia A., Bouabdallah A., Skali S.E, Ecoulement de Taylor-Couette en géométrie finie et à surface libre, *The Canadian Journal of Chemical Engineering*, 83, 652-657 (2005).
- [9] Rehimi F., Caractérisation expérimentale des structures tourbillonnaires derrière un cylindre en milieu confiné par PIV et par polarographie, PhD Thesis, University of Nantes, France (2006).
- [10] Abassi W., Investigations expérimentales et modélisations numériques par la méthode de Lattice Boltzmann (LBM) pour l'étude des transferts dans les écoulements tourbillonnaires, PhD Thesis, University of Nantes, France (2014).
- [11] Sobolik V., Jirout T., Havlica J., Kristiawan M., Wall Shear Rates in Taylor Vortex, *Journal of Applied Fluid Mechanics*, 4 (2), 25-31 (2011).